


# Nanoprobe-based mass spectrometry and Fourier transform infrared spectroscopy for rapid phospholipid profiling

Elias Gizaw Mernie<sup>1</sup> | Mei-Chun Tseng<sup>1,2</sup> | Wen-Ti Wu<sup>1</sup> | Tzu-Ming Liu<sup>3</sup> | Yu-Ju Chen<sup>1,4</sup> 

<sup>1</sup>Institute of Chemistry, Academia Sinica, Taipei, Taiwan

<sup>2</sup>Department of Chemistry, Soochow University, Taipei, Taiwan

<sup>3</sup>Institute of Translational Medicine, Faculty of Health Sciences, University of Macau, Taipa, China

<sup>4</sup>Department of Chemistry, National Taiwan University, Taipei, Taiwan

## Correspondence

Yu-Ju Chen, Institute of Chemistry, Academia Sinica, Taipei, Taiwan.  
Email: yujuchen@gate.sinica.edu.tw

## Funding information

Ministry of Science and Technology of Taiwan, Grant/Award Number: MOST-107-2113-M-001-023-MY3; Small Molecule Mass Spectrometry Facility at the Institute of Chemistry, Academia Sinica, Grant/Award Number: AS-CFII-108-109

## Abstract

Phospholipids are the major components of cellular membranes and possess important biological roles. Despite their significance in diagnosis and therapeutic application in various diseases, systematic profiling of phospholipids remains challenging due to time-consuming sample preparation and their inherent structure complexity. Taking advantages of complementary, simple, and fast structural analysis by matrix-assisted laser desorption ionization-time of flight mass spectrometry (MALDI-TOF MS) and Fourier transform infrared spectroscopy (FTIR), we reported a nanoprobe-based dual detection strategy for large-scale phospholipid profiling. Based on electrostatic interaction between nitrilotriacetic acid (NTA) chelated iron ion and phosphate head on phospholipids, we developed an NTA-decorated magnetic nanoparticle (MNP)-based strategy for enrichment of phospholipids from lung cancer cell lines. Compared to the conventional liquid-liquid extraction, NTA@MNP nanoprobe enrichment demonstrated 2.6-fold more identified phospholipids. By direct on-particle analysis, FTIR confirmed the P-O-C and phosphate stretching characteristic of the phospholipid head group, and MALDI-TOF MS identified a total of 59 phospholipids from PC9 and A549 lung cancer cells. Comparing the variation of phospholipids between two cell lines, we identified significantly more phospholipids in the PC9 cells (49) compared to 35 phospholipids in the A549 cells. The comparison also revealed 24 and 10 cell line-specific phospholipids in the PC9 and A549 cells, respectively. Given the demonstrated rapid enrichment and unambiguous identification of phospholipids at cellular levels, the developed approach can provide systematic profiling to study the under-explored phospholipid species.

## KEYWORDS

Fourier transform infrared spectroscopy, magnetic nanoparticles, matrix-assisted laser desorption ionization-time of flight mass spectrometry, phospholipids

## 1 | INTRODUCTION

Lipids are a category of structurally diverse molecules that have essential biological functions.<sup>[1]</sup> As a class of lipids, phospholipids are the major constituents of all cellular membranes.<sup>[2,3]</sup> Due to their special arrangement as a lipid bilayer to protect the interior of cells and enable selective transport processes,<sup>[4]</sup> phospholipids play important roles in the biological membranes such as energy storage, cellular signaling, membrane trafficking, and cell–cell interactions.<sup>[5,6]</sup> Imbalance and alteration of phospholipids cause serious conditions in living organisms, such as chronic inflammation, cardiovascular diseases, diabetes, and neurodegenerative diseases.<sup>[7]</sup> Structurally, phospholipids consist of a hydrophilic phosphate head group, and a hydrophobic glycerol backbone which is esterified with fatty acids.<sup>[8]</sup> The phosphate group can be modified with simple organic molecules such as choline, ethanolamine or serine while the sn-1 and sn-2 position of the glycerol.<sup>[3]</sup> Based on their polar head group modification, they are divided into subclasses including phosphatidylcholine (PC), phosphatidylethanolamine, phosphatidylserine, phosphatidylglycerol, and phosphatidylinositol.<sup>[9]</sup>

The phospholipid research has attracted much attention due to their important role in disease biomarker discovery.<sup>[10]</sup> Identification of abnormal phospholipids associated with disease nominate translational opportunity for the development of new diagnostic and therapeutics for various diseases, such as cancer, diabetes, and neurodegenerative diseases.<sup>[5,11]</sup> However, due to the inherent chemical complexity, the analysis of phospholipids and lipids is challenging and has less progress compared with other “omics” technologies.<sup>[7]</sup>

Owing to its high sensitivity and specificity, mass spectrometry (MS) is a powerful tool to characterize phospholipids.<sup>[10]</sup> Particularly, the soft-ionization techniques such as electrospray ionization and matrix-assisted laser desorption ionization (MALDI) MS have been utilized in the structural characterization of phospholipids present in biological samples for the development of novel phospholipid-based biomarkers.<sup>[5]</sup> The high-performance liquid chromatography coupled with high-resolution MS has been the most commonly used platform for phospholipid analysis.<sup>[12]</sup> Nevertheless, derivatization techniques are required to increase the ionization efficiency for phospholipid precursor ions and introduce a selective fragment for neutral loss scans.<sup>[7]</sup>

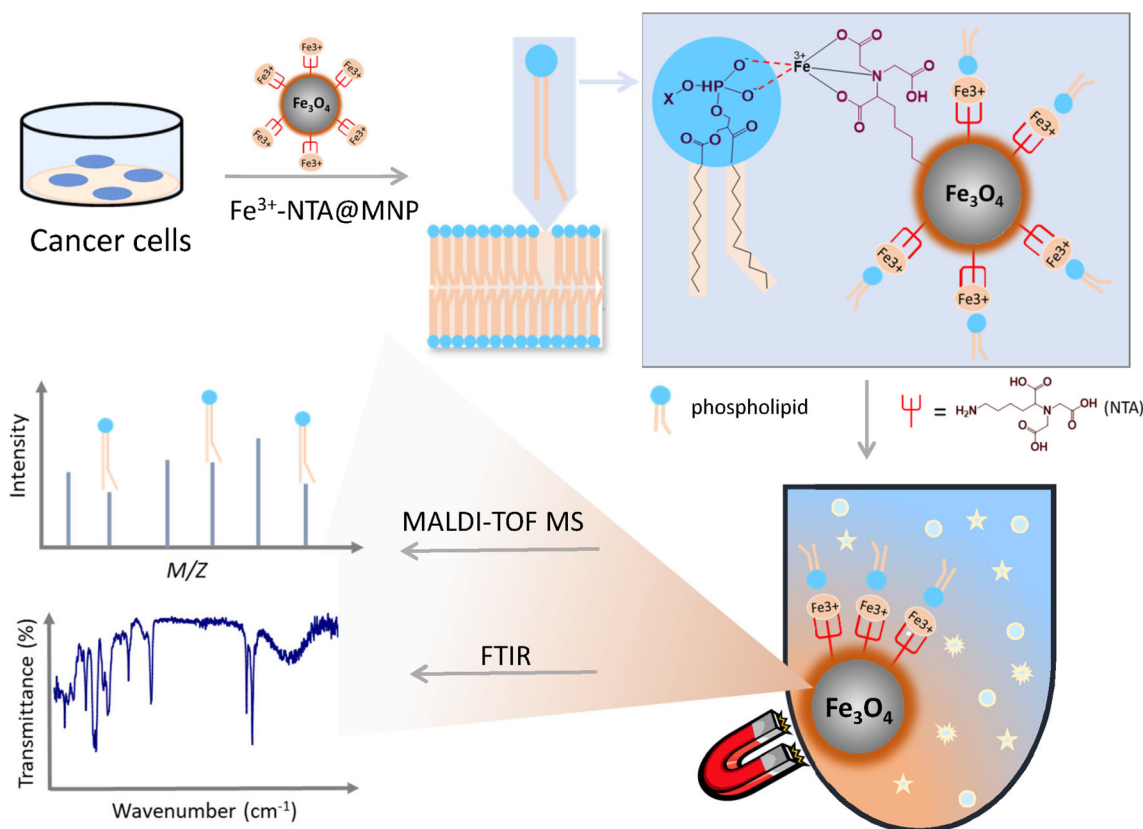
Compared to LC–MS, MALDI-TOF MS is a promising alternative technique for the analysis of phospholipids due to the instrumental robustness, speed of analysis, and high sensitivity.<sup>[10,11,13]</sup> Fuchs et al utilized the MALDI-TOF MS for the determination of spermatozoa phospholipid composition from several ruminantia and feloideae species. The

fingerprint of phospholipids species has been reported that allows the differentiation between both animal groups.<sup>[13]</sup> The various methods for analyzing phospholipids in urine have been compared and optimized from a clinical perspective. Li et al has identified a total of 31 lipid species from three lower urinary tract male patients using MALDI-TOF MS.<sup>[14]</sup> Lee et al analyzed 21 pairs of cancerous and adjacent normal tissues from 21 patients with non-small cell lung cancer (NSCLC). Several phospholipids including PC (34:1) were identified to show differentiating power between the cancer and normal tissues with 92.9% accuracy.<sup>[15]</sup> By a surface-printed microdot array chip coupled with MALDI MS, 12 phospholipids have been reported at the single-cell level and the structures were confirmed by MS/MS.<sup>[16]</sup>

Compared to above-mentioned advancements of MS methods, development of selective isolation and enrichment strategies for phospholipids has gained less attention. Liquid–liquid extraction (LLE) techniques are the most widely utilized technique for extraction of phospholipids.<sup>[17]</sup> However, there is a high risk of precipitation of contaminating compounds (salt or interference from the matrix)<sup>[6]</sup> to cause potential interference in the MS analysis. To provide a highly efficient method for selective enrichment and structural characterization of phospholipids, in this study, we report a nanoparticle-based phospholipid enrichment strategy and integrate with dual on-nanoparticle detection by spectroscopy and MS. Based on the electrostatic interaction between chelated iron ion in NTA and the phosphate head group in phospholipids, nitrilotriacetic acid conjugated magnetic nanoparticle (NTA@MNP) were designed and fabricated to enrich phospholipids from cells. The NTA@MNP offers advantages of rapid purification with magnetic collection and direct detection on nanoparticles without the need of analyte elution, which can be achieved by using Fourier transform infrared spectroscopy (FTIR) to confirm the functionality in phospholipids as well as MALDI-TOF MS to identify the molecular formulas. Using lung cancer cell line (PC9 and A549) as a model, the feasibility of the reported strategy was demonstrated on the large-scale identification of cellular phospholipids and their variation of between two cell lines.

## 2 | RESULTS AND DISCUSSION

Scheme 1 shows the integrated pipeline for nanoprobe-based phospholipid identification and characterization by MALDI-TOF MS and FTIR. First, the NTA@MNP were fabricated following our previously reported protocol.<sup>[18]</sup> Second, the NTA@MNP affinity probe was activated by ferric ion ( $\text{Fe}^{3+}$ ) which is responsible for electrostatic interaction with the phosphate head group of



**SCHEME 1** Analytical workflow of NTA@MNP-based phospholipid enrichment and structural analysis. Nitrilotriacetic acid (NTA) is conjugated onto the magnetic nanoparticle (MNP), then phospholipids were extracted and enriched from lung cancer cell lines followed by structural characterization using on-particle detection using MALDI-TOF MS and FTIR

phospholipids. Third, enrichment of phospholipids is achieved by incubation of the activated  $\text{Fe}^{3+}$ -NTA@MNP with phospholipids extract mixture. Fourth, NTA@MNP-captured phospholipids were separated from the solution by magnet, then the samples were dried and reconstituted. Finally, structural characterization of phospholipids was performed using MALDI-TOF MS and FTIR. The FTIR experiment was designed for a fast assessment of phospholipids on the NTA@MNP nanoprobe after enrichment, followed by identification and structural elucidation of the phospholipids based on the MALDI-TOF MS. All the mass spectra were acquired in positive ion mode and the online database search was utilized to facilitate and confirm the assignment of phospholipids. The LIPID MAPS online database<sup>[19,20]</sup> search result was used for MS peaks assignment and the detailed structure was also further confirmed by tandem MS analysis.

## 2.1 | Assessment of NTA@MNP for standard phospholipid enrichment

The enrichment performance of NTA@MNP nanoprobe for phospholipids was firstly evaluated by using reference

phospholipid standards. The standard solutions of two phospholipids PC(16:0/16:0) and PC(18:1/18:1) were prepared in methanol and then the enrichment was performed by mixing with NTA@MNP with 1:5 ratio. These standards are PC classes with different acyl side chains (insert structures in Figure 1a,b). The PCs were successfully enriched by NTA@MNP and the characteristic molecular ion peaks were observed in the MALDI-TOF MS spectra. The peak at  $m/z$  734.6 matched to the theoretical mass of proton adduct  $[\text{M} + \text{H}]^+$  (734.57) of PC (16:0/16:0) (Figure 1a) and the peak at  $m/z$  786.6 was assigned to PC(18:1/18:1), theoretical mass (786.60) (Figure 1b).

Compared to the MALDI-TOF MS, FTIR is a powerful alternative analytical technique for the rapid identification of functional groups.<sup>[21]</sup> The FTIR method has also been demonstrated for the identification of phospholipids from vegetable oil and plasma.<sup>[22,23]</sup> In the current study, we first prepared the pure phospholipid standard of PC(16:0/16:0) for FTIR analysis to identify the vibration bands of phospholipids. The peaks in the 900–1500  $\text{cm}^{-1}$  region were attributed to vibration bands of P-O-C and phosphate stretching in the phospholipid head group, whose results are consistent with the previous

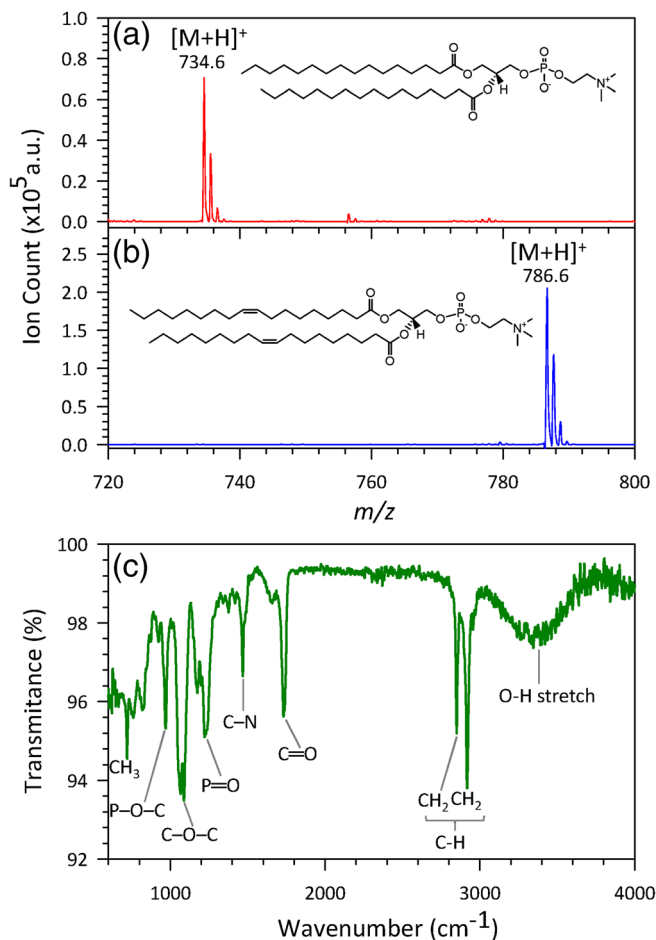


**FIGURE 1** MALDI TOF MS and FTIR spectra of reference phospholipid standards after NTA@MNP enrichment. (a) MS spectrum of 1,2-dihexadecanoyl-sn-glycero-3-phosphocholine PC (16:0/16:0). (b) MS spectrum of 1,2-di-(9Z-octadecenoyl)-sn-glycero-3-phosphocholine PC(18:1/18:1). (c) FTIR spectrum of 1,2-dihexadecanoyl-sn-glycero-3-phosphocholine PC(16:0/16:0)

studies.<sup>[22]</sup> In addition to the head group, the C-H stretching of acyl side chains lies between 2800 and 3000  $\text{cm}^{-1}$  which was fairly strong compared to other vibration bands in the head group (Figure 1c). The result indicated that phospholipids were effectively bound and isolated from the solution by the NTA@MNP nanoprobe. The clean background and high-intensity peaks illustrate that the NTA@MNP nanoprobe did not interfere in the ionization process for MS detection (Figure 1).

## 2.2 | Phospholipid enrichment and characterization from lung cancer cell lines

The feasibility of comprehensive enrichment and analysis protocols for complex samples was further evaluated for the identification of phospholipids from two lung cancer cell

lines (PC9 and A549). LLE using chloroform, methanol, and water is the conventional method for phospholipid extraction from the real sample.<sup>[24–26]</sup> To assess the performance of our nanoprobe, we compared the enrichment capability of LLE and NTA@MNP for phospholipid identification. The extracted phospholipids from the two strategies were subjected to MALDI-TOF MS analysis. All mass spectra were acquired in reflector positive ionization mode and all of the peaks are corresponding to the proton adduct. The possible structure of different phospholipids was assigned based on the intact mass matching with mass accuracy of 0.5 Da from online LIPID MAPS database search result and MS/MS fragmentation pattern. Only 19 phospholipids were detected by the conventional LLE (Figure 2a), whereas dramatically higher number of 49 phospholipids were identified using NTA@MNP enrichment (Figure 2b), corresponding to 2.6-fold more phospholipids. The comparison reveals that NTA@MNP nanoprobe-based strategy provides superior enrichment performance with higher number of identified phospholipids from the cell extract compared to the conventional LLE.

To confirm the characteristic functional group on the phospholipids, the NTA@MNP-isolated phospholipids from the PC9 cell line were also submitted to FTIR analysis. The NTA@MNP spectrum was used as a control background to eliminate the interference vibration bands from the nanomaterial. The resulting FTIR spectrum was compared with the pure standard phospholipid spectrum. Very similar FTIR spectra were observed from the cell line and the standard phospholipid (Figure 2c). The strong pair of vibration bands between 2800 and 3000  $\text{cm}^{-1}$  was due to the C-H stretching of the acyl side chains, and the peaks in the region below 2000  $\text{cm}^{-1}$  indicated the vibration bands of the head group stretching. Particularly, vibration bands at 1740, 1470, and 1070  $\text{cm}^{-1}$  represented the C=O, C-N, and P-O-C stretching, respectively. Taken together, results from both the MALDI-TOF MS and FTIR results demonstrated the effective isolation of phospholipids from the cell line matrix by using the NTA@MNP nanoprobe. The FTIR result unambiguously confirmed the characteristic phosphate functional group, while MS complementarity identified the different unknown phospholipid species. Overall, NTA@MNP nanoprobe-based MALDI-TOF MS and FTIR profiling successfully revealed the phospholipid composition in the human cancer cell lines.

## 2.3 | MALDI-TOF MS/MS for phospholipid structural elucidation

The detailed structural determination of identified phospholipids was conducted using MALDI-TOF MS/MS fragmentation. First, the MS/MS of the two reference

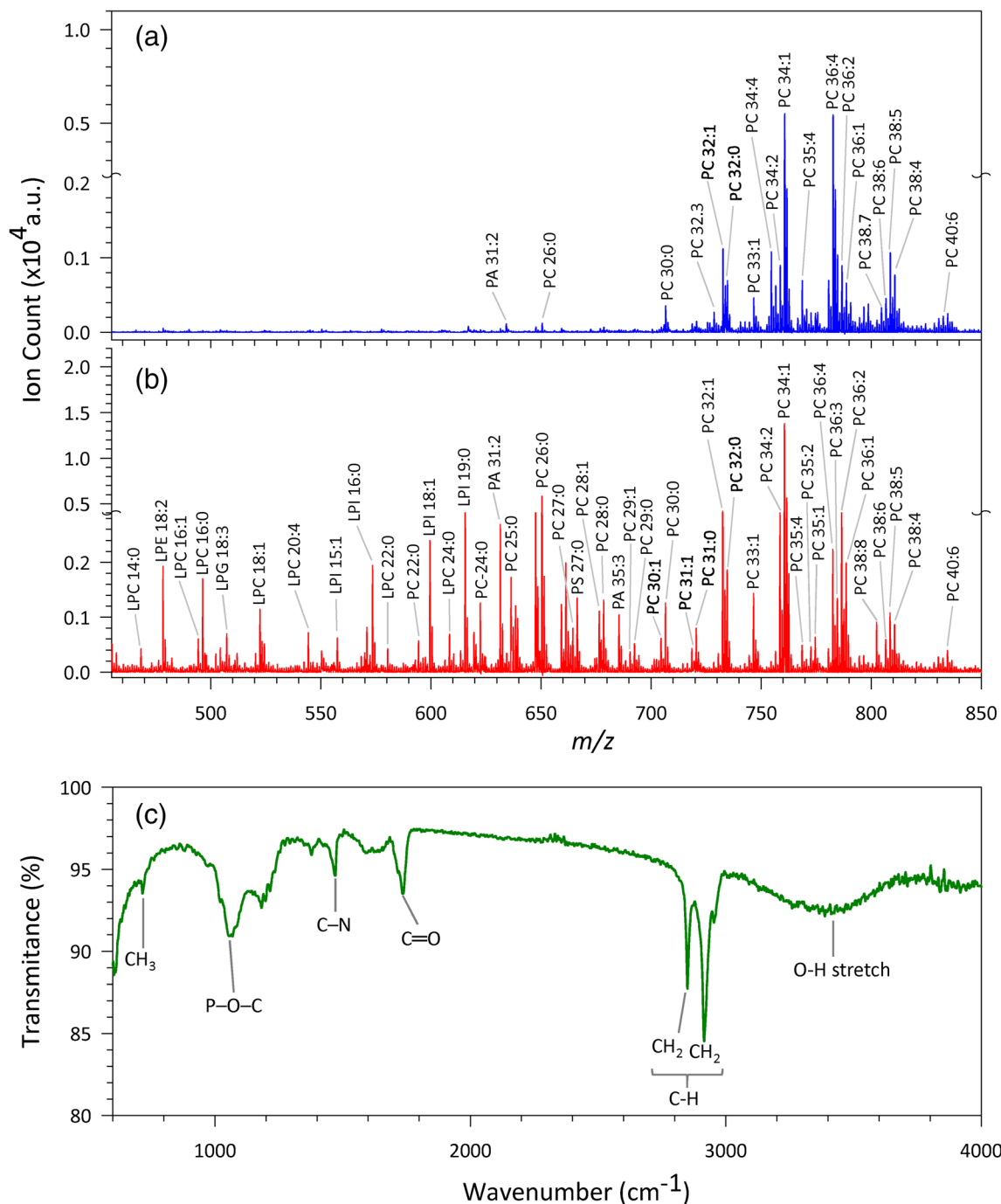


**FIGURE 2** Representative positive ion MALDI-TOF mass spectra and FTIR spectra of the extracted phospholipids from PC9 cancer cell line. (a) MALDI-TOF mass spectrum of phospholipids after NTA@MNP enrichment. (b) MALDI-TOF mass spectrum of phospholipids extract following the conventional chloroform—methanol ( $\text{CHCl}_3$ -MeOH, 2:1 vol/vol) liquid-liquid extraction. (c) FTIR spectrum of phospholipids after NTA@MNP enrichment from PC9 cell line

standards (PC(16:0/16:0) and PC(18:1/18:1)) were performed to evaluate the fragmentation pattern of phospholipids in MALDI-TOF MS/MS. The result shows both standards produced a moderate degree of fragmentation from the precursor ions. The fragment ions were commonly found in two  $m/z$  regions (Figure 3). The major peaks in the lower mass range ( $m/z < 200$ ), including

$m/z$  86.0, 104.1, 147.0, and 184.1 and 198.1, correspond to the phospholipid head group fragmentation (Figure 3), in the higher mass region ( $m/z > 400$ ), signature fragments can be assigned to identify the phospholipid structure, including  $m/z$  478.3, 496.3, and 551.4 from PC(16:0/16:0) fragmentation (Figure 3a), as well as  $m/z$  504.3, 522.3, and 603.5 ion from PC(18:1/18:1) from the cleavage of

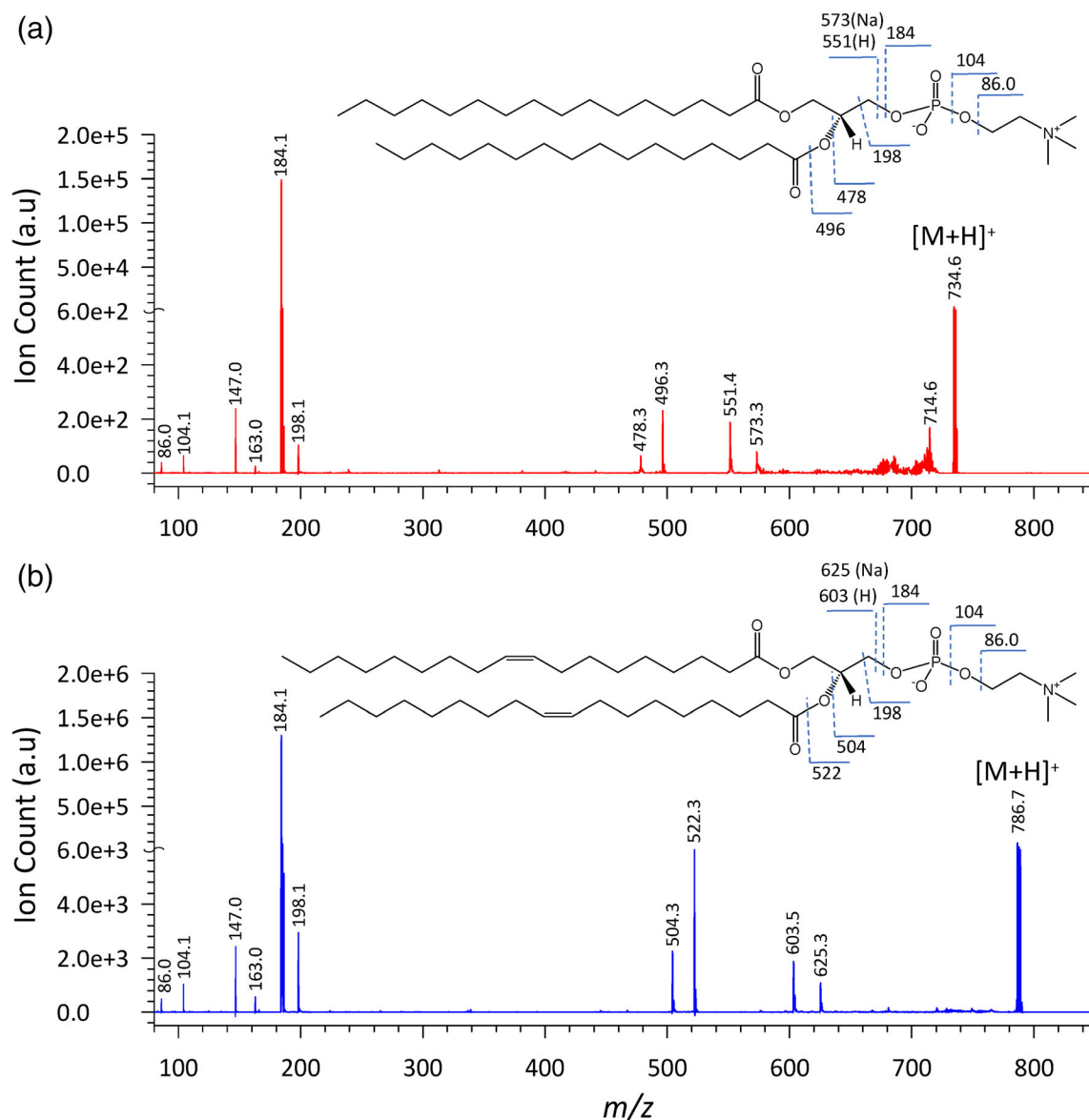
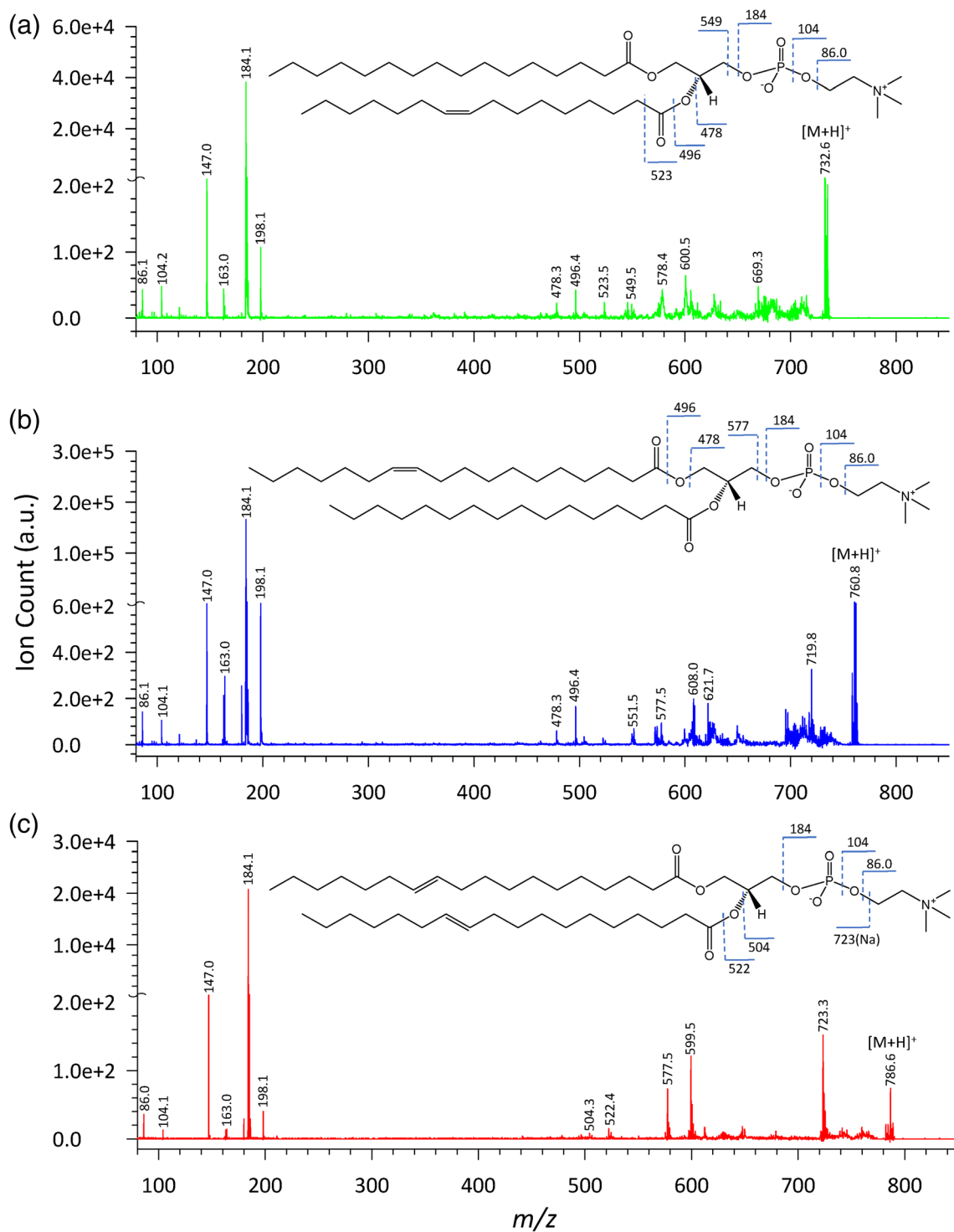


FIGURE 3 MALDI-TOF MS/MS spectra of reference phospholipid standards recorded in the positive ionization mode. (a) PC(16:0/16:0). (b) PC(18:1/18:1)

bonds in glycerol (sn1, sn2, and sn3) (Figure 3b). Previous studies also demonstrated a similar fragmentation pattern (86.0, 104.1, 147.0, and 184.1 fragments) of phospholipids.<sup>[27]</sup> The fragment ions in the lower mass range provide information about the possible head group modification. In addition, the prediction of the acyl fatty acid chain length and unsaturation was enabled by the detection of fragment ions in the sn1, sn2, and sn3 of glycerol.

In the spectra of PC(16:0/16:0) (Figure 3a), the base peak at  $m/z$  184.1 corresponds to the cleavage of the phosphocholine head group. The fragment ion at  $m/z$  147 was produced by the neutral loss of 59 from the sodium adduct of the dominant fragment ion at  $m/z$  184.1. The fragment ion at  $m/z$  104.1 was formed through a loss of a phosphate group from the choline head group.

A further loss of water from ions at  $m/z$  104.1 resulted in a protonated fragment at  $m/z$  86.0 (Figure 3). These fragment ions are considered as characteristic fragment ions for PC and phosphatidylcholine (LPC).<sup>[6,28]</sup> The two reference standards are the same class and have the same head groups. As a result, identical fragment ions were observed in the low mass range. However, due to acyl side chain difference, the two standards produced different fragment ions in the higher mass range (Figure 3a,b). The fragment ions of PC(16:0/16:0) at  $m/z$  551.4 (proton adduct) and 573 (sodium adduct) indicate the length of the side chains. Most importantly, the two fragments at  $m/z$  478.3 and 496.3 were critical to differentiate the possible combination of the two side-by-side chains of fatty acid (tails) (Figure 3a). Similar information has also



**FIGURE 4** Representative MALDI-TOF MS/MS spectra of phospholipids extracted from the lung cancer cell line extract. (a) PC 32:1,  $m/z$  732.6. (b) PC 34:1,  $m/z$  760.6. (c) PC 36:2  $m/z$  786.6

prevailed in the second standard MS/MS spectrum. The peaks at 603.5 (proton adduct) and 625 (sodium adduct) provide information about the length of PC(36:2) side chains. In addition, the evidence from  $m/z$  504.3 and 522.3 fragment ions can be utilized to discriminate the side chain arrangement PC(18:1/18:1) (Figure 3b).

Therefore, MS/MS spectra provide information about the possible combination of acyl chains that are attached to the head group.

Similar to the phospholipid standards, the representative MS/MS spectra of selected precursors detected in the lung cancer cell lines are demonstrated in Figure 4. Very

strong fragment ions at  $m/z$  184.1 and other fragments in lower mass range ( $m/z$  86.1, 104.2, 147.0) were observed in all the three precursor ions, which confirm the annotation of selected phospholipid molecular ions for PC. The other fragment ions in the higher mass range also indicate some information about the possible side chains (Figure 4). From the MS spectra and the fragment ion at  $m/z$  549.5, the precursor  $m/z$  732.6 was matched with the PC 32:1 structure. Furthermore, the three fragment ions at  $m/z$  478.3, 496.4, and 523.5 suggest that the PC(16:0/16:1) was the possible side chain combination (Figure 4a). Likewise, the side chain arrangement of PC(18:1/16:0) and PC(18:1/18:1) were assigned for precursors at  $m/z$  760.8 and 786.6, respectively (Figure 4b,c). Despite the challenge in structural discrimination of several isomers of phospholipids,<sup>[27]</sup> the possible structure of phospholipids was identified after careful examination of the MS/MS fragment ions. However, the detailed characterization of released acyl side chains such as the position of double bonds is still a major bottleneck of MALDI-TOF MS due to the extremely high energy barrier of C-C bond cleavage from the acyl side chains.<sup>[10]</sup>

## 2.4 | Differential phospholipid profiles among lung cancer cell lines

To demonstrate the application of the dual detection platform, two lung cancer cell lines (PC9 and A549) were selected to compare the variation of phospholipid compositions within different cancer cells. First, the MALDI-TOF MS peaks were searched against the LIPID MAPS structure database, then the best match structures were selected based on the mass accuracy. Further structural information on the types of phospholipid and the possible side-chain compositions were assigned according to the MS/MS fragment ions produced in the head group and glycerol backbone. Overall, 59 phospholipids were identified and all phospholipids found in both lung cancer cell lines are listed in Table 1. As shown in the summary and comparison of identified phospholipids in the two cancer cell lines (Figure 5), PC is the major component in both cell lines which covers 30 identified phospholipids of all identified results (50.8%), followed by 11 LPC species (18.6%). Other phospholipid species are relatively less abundant in both the cells. The current finding is aligned with previous studies that PC is a major phospholipid species that covers approximately 40% of all eukaryotic cellular membranes.<sup>[4,29]</sup> Compared to the previous study that 28 PC and 17 LPC species were identified from the human red blood cells,<sup>[28]</sup> comparable results were obtained by enrichment by NTA@MNP and MALDI-TOF MS and LC-MS/MS analysis. Based on the

advantage of rapid enrichment by NTA@MNP, our method can be used for quick screening of phospholipids without using the conventional time-consuming phospholipids extraction techniques. Comparing the variation of phospholipids between two cell lines, we observed a different trend on the number of phospholipids (Figure 5b). In the PC9 cells, more phospholipids (49) were identified, compared to 35 phospholipids detected in the A549 cells. On the other hand, slightly more Lysophosphatidylcholine<sup>[8]</sup> were identified in the A549 cells compared to PC9 cells.<sup>[7]</sup> Besides the common 25 phospholipids, interestingly, 24 and 10 cell line-specific phospholipids were observed in the PC9 and A549 cells, respectively (Figure 5b). These results revealed different profiles in different cell lines although both cells derive from the same origin of lung cancer. Due to their functional role in the pathogenesis of various diseases such as diabetes and cancer,<sup>[28]</sup> the identified phospholipids may provide insight for further studies. To delineate the comprehensive profiles for endogenous phospholipids, systemic analysis from different cells and disease types will be required.

## 3 | EXPERIMENTAL

### 3.1 | Fabrication of NTA@MNP nanoprobe

The NTA@MNP was fabricated following the previously reported method.<sup>[18]</sup> Briefly, the core  $\text{Fe}_3\text{O}_4$  MNPs (120 mg) obtained by alkaline hydrolysis of  $\text{Fe}^{3+}$  and  $\text{Fe}^{2+}$  were coated with silane with tetraethyl orthosilicate (TEOS 0.1 ml) in ammonia solution (33%, 1.6 ml), followed by surface blocking with a mixture of 3-Aminopropyl trimethoxy silane (APS) and polyethylene glycol-400 (PEG) (20:1, 0.4 ml: 20  $\mu\text{l}$ ). The PEG-blocked MNP (15 mg) was functionalized with suberic acid bis (N-hydroxy-succinimide ester [DSS] [75 mg]) then decoration of the material with Na,Na-bis (carboxy methyl)-L-lysine hydrate (NTA) (206 mM). Finally, magnetic separation, the supernatant was removed and the particles were washed three times with deionized water. The NTA@MNP particle was suspended in deionized water and stored at 4°C for future use.

### 3.2 | Cell culture

The human lung adenocarcinoma PC9 and A549 cell lines were cultured in RPMI-1640 medium supplemented with fetal bovine serum (FBS) (10% vol/vol), sodium bicarbonate (2% wt/vol), 1 mM sodium pyruvate, 1% penicillin G (GibcoBRL, Gaithersburg, MD), and 100  $\mu\text{g}/\text{ml}$



TABLE 1 The list of all detected phospholipids from PC9 and A549 lung cancer cell lines

No.	Experimental <i>m/z</i>	Theoretical <i>m/z</i>	Formula	Name	PC9	A549
1	464.4	464.28	C22H42NO7P	LPE 17:2		v
2	468.4	468.31	C22H46NO7P	LPC 14:0	v	
3	478.4	478.29	C23H44NO7P	LPE 18:2	v	v
4	494.4	494.32	C24H48NO7P	LPC 16:1	v	
5	496.4	496.34	C24H50NO7P	LPC 16:0	v	v
6	504.4	504.31	C25H46NO7P	LPE 20:3	v	v
7	506.4	506.32	C25H48NO7P	LPC 17:2		v
8	507.3	507.27	C24H43O9P	LPG 18:3	v	
9	522.4	522.36	C26H52NO7P	LPC 18:1	v	v
10	524.4	524.37	C26H54NO7P	LPC 18:0		v
11	544.4	544.34	C28H50NO7P	LPC 20:4	v	
12	550.4	550.39	C28H56NO7P	LPC 20:1		v
13	557.5	557.27	C24H45O12P	LPI 15:1	v	
14	566.4	566.42	C29H60NO7P	LPC 21:0		v
15	573.5	573.30	C25H49O12P	LPI 16:0	v	
16	580.4	580.43	C30H62NO7P	LPC 22:0	v	v
17	594.4	594.41	C30H60NO8P	PC 22:0	v	v
18	599.6	599.32	C27H51O12P	LPI 18:1	v	
19	608.4	608.47	C32H66NO7P	LPC 24:0	v	v
20	615.6	615.35	C28H55O12P	LPI 19:0	v	
21	622.5	622.44	C32H64NO8P	PC 24:0	v	v
22	624.5	624.39	C30H58NO10P	PS 24:0		v
23	631.6	631.43	C34H63O8P	PA 31:2	v	
24	636.5	636.46	C33H66NO8P	PC 25:0	v	v
25	638.5	638.40	C31H60NO10P	PS 25:0	v	v
26	639.4	639.40	C35H59O8P	PA 32:5	v	
27	650.5	650.48	C34H68NO8P	PC 26:0	v	v
28	656.5	656.43	C35H62NO8P	PE 30:4		v
29	664.5	664.49	C35H70NO8P	PC 27:0	v	v
30	666.5	666.43	C33H64NO10P	PS 27:0	v	v
31	676.5	676.49	C36H70NO8P	PC 28:1	v	
32	678.5	678.51	C36H72NO8P	PC 28:0	v	v
33	680.5	680.45	C34H66NO10P	PS 28:0		v
34	685.5	685.48	C38H69O8P	PA 35:3	v	
35	690.5	690.51	C37H72NO8P	PC 29:1	v	
36	692.5	692.52	C37H74NO8P	PC 29:0	v	
37	694.6	694.47	C35H68NO10P	PS 29:0		v
38	704.5	704.52	C38H74NO8P	PC 30:1	v	
39	706.6	706.54	C38H76NO8P	PC 30:0	v	v
40	718.6	718.54	C39H76NO8P	PC 31:1	v	v
41	720.6	720.55	C39H78NO8P	PC 31:0	v	v
42	732.6	732.55	C40H78NO8P	PC 32:1	v	v
43	734.6	734.57	C40H80NO8P	PC 32:0	v	v

(Continues)

TABLE 1 (Continued)

No.	Experimental $m/z$	Theoretical $m/z$	Formula	Name	PC9	A549
44	746.6	746.57	C41H80NO8P	PC 33:1	v	v
45	758.6	758.57	C42H80NO8P	PC 34:2	v	v
46	760.6	760.59	C42H82NO8P	PC 34:1	v	v
47	768.6	768.55	C43H78NO8P	PC 35:4	v	
48	772.6	772.59	C43H82NO8P	PC 35:2	v	
49	774.6	774.60	C43H84NO8P	PC 35:1	v	v
50	782.6	782.57	C44H80NO8P	PC 36:4	v	v
51	784.6	784.59	C44H82NO8P	PC 36:3	v	
52	786.6	786.60	C44H84NO8P	PC 36:2	v	v
53	788.6	788.62	C44H86NO8P	PC 36:1	v	
54	798.6	798.60	C45H84NO8P	PC 37:3		v
55	802.5	802.54	C46H76NO8P	PC 38:8	v	
56	806.6	806.57	C46H80NO8P	PC 38:6	v	
57	808.6	808.59	C46H82NO8P	PC 38:5	v	
58	810.6	810.60	C46H84NO8P	PC 38:4	v	
59	834.6	834.60	C48H84NO8P	PC 40:6	v	

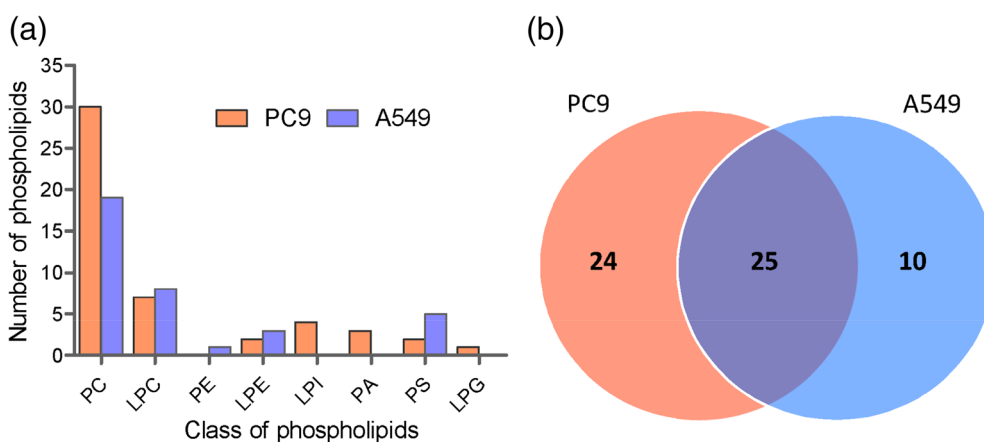


FIGURE 5 Comparison of the classes and number of phospholipids identified in two lung cancer cell lines. (a) The distribution of detected phospholipids in class. (b) The Venn diagram of identified phospholipids in PC9 and A549 cancer cell lines

streptomycin at 37°C in a humidified 5% CO<sub>2</sub>/95% air. Cells were washed three times with phosphate-buffered saline (PBS, 0.01 M sodium phosphate, 0.14 M NaCl, pH 7.4) (Sigma, St Louis, MO) and harvested.

### 3.3 | Phospholipid extraction procedure

Phospholipids were extracted using liquid-liquid extraction following the Folch procedure.<sup>[27]</sup> Briefly, the ice-cold chloroform and methanol (2:1, vol/vol) were added to the pellet cells and the sample was suspended. The suspension was vortexed occasionally to bring about physical mixing and the sample was incubated on ice for 30 min. After the addition of water, which was used to separate the aqueous and organic layers, the suspension

was incubated on ice for an additional 10 min. Samples were centrifuged at 2000 rpm for 5 min at 4°C. The lower phase (organic) layer was transferred to a new tube. The aqueous layer was re-extracted with 1 ml of 2:1, vol/vol chloroform/methanol. The chloroform layers were combined for analysis.<sup>[16]</sup>

### 3.4 | Phospholipid enrichment protocol

Ninety micrograms (90 µg) NTA@MNP were activated with Fe<sup>3+</sup> ion by adding 120 µl of 2.5 mM of FeCl<sub>3</sub> with 0.1 M ammonium acetate (NH<sub>4</sub>OAc) in 100 µl acetic acid-dd H<sub>2</sub>O solution (pH = 5–7) and mixed for 80 min. The activated Fe<sup>3+</sup>-NTA@MNP was further incubated with phospholipid extract for 100 min, and the

phospholipid bind Fe<sup>3+</sup>-NTA@MNP complexes were separated by magnet, dried in speed vac, and re-constituted in 10  $\mu$ l 50% acetonitrile/0.1% trifluoroacetic acid solution. One microliter of the reconstituted sample was mixed with 1  $\mu$ l of DHB matrix directly on the MALDI target, dried, and analyzed in MALDI-TOF MS instrument.

### 3.5 | MALDI-TOF mass spectrometry

All the mass spectra were acquired on a Bruker, New ultrafleXtremeTM, mass spectrometer (Bruker Daltonics, Bremen, Germany) equipped with an Nd-YAG laser (255 nm) operating at a repetition rate of 200 Hz. The spectra were recorded in reflectron mode using an accelerating voltage of 20 kV and a grid voltage of 16 kV in the MS/MS mode using CID gas (air). For accurate mass measurements, the instrument was calibrated with known standards polyethylene glycol (PEG) and Angiotensin 1 for MS and MS/MS, respectively. The MS/MS measurements were conducted using a collision energy of 1 kV and a CID gas pressure of  $3.7 \times 10^{-6}$  Torr. A typical mass spectrum was obtained by averaging 2000 laser shots, and the data were processed and analyzed with the Flex Analysis software 3.4 (Bruker, Daltonics).

## 4 | CONCLUSIONS

In the present study, we demonstrated a nanoparticle-based phospholipid enrichment strategy with dual detection by FTIR spectroscopy and MS for large-scale structural characterization of phospholipids in the cancer cell lines. The iron-activated NTA@MNP material provides a rapid and facile sample preparation for extraction of endogenous phospholipids. It is the first time that complementary FTIR and MS were used for rapid characterization and further structural assignment, respectively. Although the FTIR cannot provide complete structural information of unknown compounds in the complex sample, it is a rapid method to identify the P-O-C and phosphate stretching which are characteristics of phospholipids. Though the selective enrichment of phospholipids is based on the generic electrostatic affinity of the iron-activated NTA@MNP with the phosphate head group, such affinity and following washing and MALDI MS steps may potentially favor stronger binder or detectable species. As a result, the lower molecular weight phospholipids like LPCs were identified after enrichment. Despite LC-MS/MS has been commonly used for the separation and profiling of phospholipids, our approach offers the advantage of fast screening of phospholipids without derivatization and retention time

profiling. Given the demonstrated efficiency in rapid enrichment and unambiguous identification of phospholipids at cellular levels, we expect that the reported approach can be applied to other sample types to study the under-explored phospholipid species.

### ACKNOWLEDGMENTS

This research was supported by grants from the Ministry of Science and Technology of Taiwan (MOST-107-2113-M-001-023-MY3) and the Small Molecule Mass Spectrometry Facility at the Institute of Chemistry, Academia Sinica (AS-CFII-108-109).

### CONFLICT OF INTEREST

The authors declare no competing financial interests.

### ORCID

Yu-Ju Chen  <https://orcid.org/0000-0002-3178-6697>

### REFERENCES

- [1] E. Fahy, D. Cotter, M. Sud, S. Subramaniam, *Biochim. Biophys. Acta* **2011**, *1811*, 637.
- [2] W. Dong, Q. Shen, J. T. Baibado, Y. Liang, P. Wang, Y. Huang, Z. Zhang, Y. Wang, H.-Y. Cheung, *Int. J. Mass Spectrom.* **2013**, *343–344*, 15.
- [3] S. Drescher, P. van Hoogevest, *Pharmaceutics* **2020**, *12*, 1235.
- [4] K. M. Engel, J. Schiller, *Chem. Phys. Lipids* **2017**, *203*, 33.
- [5] R. Bandu, H. J. Mok, K. P. Kim, *Mass Spectrom. Rev.* **2018**, *37*, 107.
- [6] M. Frick, T. Hofmann, C. Haupt, C. Schmidt, *Anal. Bioanal. Chem.* **2018**, *410*, 4253.
- [7] T. Zullig, M. Trotschmuller, H. C. Kofeler, *Anal. Bioanal. Chem.* **2020**, *412*, 2191.
- [8] M. Alagumuthu, D. Dahiya, P. Singh Nigam, *AIMS Mol. Sci.* **2019**, *6*, 1.
- [9] E. Fahy, S. Subramaniam, H. A. Brown, C. K. Glass, A. H. Merrill Jr., R. C. Murphy, C. R. Raetz, D. W. Russell, Y. Seyama, W. Shaw, T. Shimizu, F. Spener, G. van Meer, M. S. VanNieuwenhze, S. H. White, J. L. Witztum, E. A. Dennis, *J. Lipid Res.* **2005**, *46*, 839.
- [10] B. Fuchs, C. Schober, G. Richter, R. Suss, J. Schiller, *J. Biochem. Biophys. Methods* **2007**, *70*, 689.
- [11] G. Stubiger, M. Wuczkowski, W. Bicker, O. Belgacem, *Anal. Chem.* **2014**, *86*, 6401.
- [12] M. Holcapek, G. Liebisch, K. Ekroos, *Anal. Chem.* **2018**, *90*, 4249.
- [13] B. Fuchs, U. Jakop, F. Goritz, R. Hermes, T. Hildebrandt, J. Schiller, K. Muller, *Theriogenology* **2009**, *71*, 568.
- [14] X. Li, K. Nakayama, T. Goto, S. Akamatsu, K. Shimizu, O. Ogawa, T. Inoue, *Chem. Phys. Lipids* **2019**, *223*, 104787.
- [15] G. K. Lee, H. S. Lee, Y. S. Park, J. H. Lee, S. C. Lee, J. H. Lee, S. J. Lee, S. R. Shanta, H. M. Park, H. R. Kim, I. H. Kim, Y. H. Kim, J. I. Zo, K. P. Kim, H. K. Kim, *Lung Cancer* **2012**, *76*, 197.
- [16] T. Yang, D. Gao, F. Jin, Y. Jiang, H. Liu, *Rapid Commun. Mass Spectrom.* **2016**, *30*(Suppl 1), 73.
- [17] Z. Liu, S. Rochfort, B. G. Cocks, *J. Chromatogr. A* **2016**, *1458*, 145.

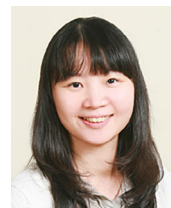
- [18] H. T. Wu, C. C. Hsu, C. F. Tsai, P. C. Lin, C. C. Lin, Y. J. Chen, *Proteomics* **2011**, *11*, 2639.
- [19] E. Fahy, M. Sud, D. Cotter, S. Subramaniam, *Nucleic Acids Res.* **2007**, *35*, W606.
- [20] M. Sud, F. E. Fau, D. Cotter, C. D. Fau, A. Brown, B. A. Fau, E. A. Dennis, D. E. Fau, C. K. Glass, G. C. Fau, A. H. Merrill, Jr., F. Merrill Ah Jr, R. C. Murphy, M. R. Fau, C. R. H. Raetz, R. C. Fau, D. W. Russell, R. D. Fau, S. Subramaniam, S. Subramaniam. LMSD: LIPID MAPS Structure Database.
- [21] C. Berthomieu, R. Hienerwadel, *Photosynth. Res.* **2009**, *101*, 157.
- [22] J. M. Nzai, A. Proctor, *J. Am. Oil Chem. Soc.* **1998**, *75*, 1281.
- [23] A. Oleszko, S. Olsztyńska-Janus, T. Walski, K. Grzeszczuk-Kuc, J. Bujok, K. Galecka, A. Czerski, W. Witkiewicz, M. Komorowska, *Biomed. Res. Int.* **2015**, *2015*, 245607.
- [24] B. E. Fau, W. J. Dyer, W. J. Dyer, *Can. J. Biochem. Physiol.* **1959**, *37*, 911.
- [25] J. Folch, M. Lees, G. H. S. Stanley, *J. Biol. Chem.* **1957**, *226*, 497.
- [26] H. Zhang, Y. Gao, J. Sun, S. Fan, X. Yao, X. Ran, C. Zheng, M. Huang, H. Bi, *Anal. Bioanal. Chem.* **2017**, *409*, 5349.
- [27] J. J. Jones, S. M. Batoy, C. L. Wilkins, *Comput. Biol. Chem.* **2005**, *29*, 294.
- [28] F. Xu, L. Zou, Q. Lin, C. N. Ong, *Rapid Commun. Mass Spectrom.* **2009**, *23*, 3243.
- [29] V. Vassar, C. Hagen, J. Ludwig, R. Thomas, J. Zhou, *Bio-techniques* **2007**, *42*, 442.

## AUTHOR BIOGRAPHIES



**Elias Gizaw Mernie** received his M. Sc. degree from Addis Ababa University, Ethiopia in 2011 and Ph.D. degree from National Taiwan University of Science and Technology, Taiwan in 2020 under the supervision of Prof. Yu-Ju Chen. Elias's Ph. D. dissertation focused on direct coupling of high-performance thin-layer chromatography (HPTLC) separation technique with 2,5-dihydroxybenzoic acid conjugated magnetic nanoparticle (DHB@MNP) matrix-assisted laser desorption ionization time-of-flight (MALDI-TOF) mass spectrometry (MS) for simultaneous glycans separation and structural elucidation. In his Ph.D. work, Elias demonstrated the potential capability of ionic liquids as dispersant and stabilizing agent for homogeneous coating of DHB@MNP nanomatrix on the TLC surface. He successfully applied this approach for direct analysis of human milk oligosaccharides (HMOs) and has published his work in the *Analytical Chemistry*. He currently works as a postdoctoral research fellow at the Institute of Chemistry, Academia Sinica. Since he started his postdoctoral, he developed a method to resolve the structures of more challenging heparin-

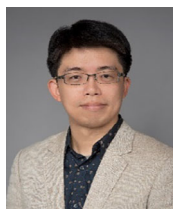
like glycosaminoglycans and glycoproteome using MALDI-TOF MS and liquid chromatography-electrospray ionization (LC-ESI)-Ion Mobility MS. He also fabricated and applied the novel nitrilotriacetic acid-decorated magnetic nanoparticle and zwitterionic hydrophilic interaction liquid chromatography (cHILIC) nanoparticle-based strategy for enrichment and analysis of various biomolecules. His current research focuses on porphyrin profiling and coupling of LC-MS/MS with data-independent acquisition methods for glycoprotein identification.



**Mei-Chun Tseng** received Ph.D. from National Taiwan University in January 2004 under the supervision of Prof. Guor-Rong Her. Her Ph.D. dissertation focused on the electrospray ionization mechanism and MALDI-TOF MS application, wherein we have successfully developed several new interfaces for the CE-MS applications to improve sensitivity and salt tolerance. After obtaining her degree, she was offered a postdoctoral research fellow position at Academia Sinica in 2004 to take charge of the operation of the mass spectrometry facility. To create a state-of-the-art core facility for the significantly increasing demand for analytical services, Academia Sinica offered her position as an assistant research specialist, in 2005 and is currently a senior research specialist (since 2016). She also currently holds adjunct associate professorships at Soochow University. She has established a variety of mass spectrometry-based pipelines providing services for quality analysis ranging from identification of compounds to structure determination to the quantification of analytes. New technologies in sample pretreatment or instrumentation have been also jointly developed with users to address the unmet needs of their research in diverse fields. Thus, the number of services has increased significantly to reach >12,000 samples a year from Academia Sinica users as well as university and industry ones. Her work has been published in 37 articles with co-authors, including *Angew. Chem. Int. Ed.*, *Chem. Commun.*, *Cancer Cell*, *Chem. Sci.*, *Anal. Chem.*, *Cell Reports*, *ACS Catal.*; especially two papers published in *Chemical Science* and *J. Am. Soc. Mass Spectrom.* as first author and one paper published in *Analytical Chemistry* as the co-corresponding author and 1 book chapter including co-editing a best-selling mass spectrometry textbook in Chinese. She is also the Elected Council Member of *Taiwan Society for Mass Spectrometry* (2014–2021).



**Wen-Ti Wu** starts to work in the Institute of Chemistry, Academia Sinica, manage photovoltaic and material analysis core facilities in 2014. These include large-area emerging photovoltaic solar cells fabrication, solar energy conversion efficiency, both optical and electrical interfacial kinetic analysis and material characteristics. She demonstrates that novel materials developed by our PIs applied into large-area solar modules, and further integrated with low-power consumption products, such as iBeacon, electronic calculator, and temperature sensor, stability filed test of the prototypes monitoring more than 5 years. Based on this performance these materials are promising to develop solar cells/modules for next 5G era's internet of things application.



**Tzu-Ming Liu** received his B.S. degree in Electrical Engineering from National Taiwan University in 1999 and the Ph.D. degrees in Photonics & Optoelectronics from National Taiwan University in 2004. When he was a Ph.D. student, he built high-power femtosecond laser systems to study nonlinear optics. Throughout the postdoctoral research period between 2005 and 2009, he further applied femtosecond laser techniques in the studies of phonon physics, nanophotonics, and embryo development. He built miniaturized nonlinear optical microscopes based on scanning MEMS mirrors. Dr. Liu was an assistant professor since 2009 and became an associate professor in the Institute of Biomedical Engineering, National Taiwan University. He developed 800–2300 nm infrared femtosecond lasers to perform nonlinear optical microscopy in vivo and medical spectroscopy in situ. Based on this multidimension analytic platform, he achieved harmonic generation-based in vivo imaging flow cytometry in human blood vessels. He also developed quantitative indices to analyze remodeling of tumor collagen and disordered bilirubin metabolism in cancers. In 2012, he visited Wellman Center for Photomedicine, Massachusetts General Hospital in United States and built multicolor infrared femtosecond laser sources for multi-label multiphoton microscopy. In 2016, he moved to University of Macau as Associate Professor. He extended his multidimension imaging platform with functional probes and transgenic labeled mice to study the complicated cellular and molecular dynamics in the disease animal model. Topics include the niche environment of cancer stem cells, the activation status of macrophage in vivo, and

the diagnosis of cytokine storm through medical spectroscopy.



**Yu-Ju Chen** obtained her B.S. in chemistry from National Taiwan University (1992) and Ph.D. degree from Prof. Cheuk-Yiu Ng's group at Iowa State University (1997). After short postdoctoral research work at the Ames Laboratory, United States (1997), she joined Prof. Yuan-Pern Lee's group at National Tsing Hua University (1999), Dr. Chen joined the Institute of Chemistry of Academia Sinica in 1999 and is currently a Distinguished Research Fellow (2019) and Director (2013–2021). She also currently holds concurrent adjunct professorships at few universities, including National Taiwan University, National Ocean University. With great passion to reveal disease network, she is one of the pioneering scientists in establishing mass spectrometry-based proteomics in Taiwan and Asia. Her research focuses on methodology development by integrating novel nanomaterial, advanced mass spectrometry and bioinformatics. In particular, she is interested in applying these tools for in-depth exploration of the under-represented membrane proteome and post-translational modification and their application to delineate the proteome network in biology and diseases. Her work has been published in >150 articles, including *Cell*, *Mol. Cell*, *Proteomics*, *J. Proteome Res.*, *Anal. Chem.*, *JACS.*, *Nat. Commun.*, *Cancer Cell*, *Plant Cell* and *PNAS*, and 5 book chapters including co-editing a best-selling mass spectrometry textbook in Chinese (2,500+ copies sold since 2015). She has played a key role to actively promote proteomics research and networking in domestic and international community. She is Associate Editor of “*Analytical Chemistry*,” Editorial Board of “*Proteomics*” and “*Journal of Proteome Research*.” She has been the President of the Taiwan Proteomics Society (2009–2011), President of *Taiwan Society for Mass Spectrometry* (2011–2013). She is also the Vice President (2017–2019) and Council Member of AOHUPO. She is now the President of Human Proteome Organization (HUPO, the largest international proteomics society, 2021–2022), and Vice President of the Chinese Chemical Society located in Taipei (2021–2022).

**How to cite this article:** E. G. Mernie, M.-C. Tseng, W.-T. Wu, T.-M. Liu, Y.-J. Chen, *J. Chin. Chem. Soc.* **2021**, *1*, <https://doi.org/10.1002/jccs.202100284>